Neutron Spectroscopic Factors in ^{9}Li from ^{2}H(^{8}Li, p)^{9}Li

A. H. Wuosmaa,[1] K. E. Rehm,[2] J. P. Greene,[2] D. J. Henderson,[2] R. V. F. Janssens,[2] C. L. Jiang,[2] L. Jisonna,[3] E. F. Moore,[2] R. C. Pardo,[2] M. Paul,[4] D. Peterson,[2] Steven C. Pieper,[2] G. Savard,[2] J. P. Schiffer,[2] R. E. Segel,[3] S. Sinha,[2] X. Tang,[2] and R. B. Wiringa[2]

[1]*Physics Department, Western Michigan University, Kalamazoo, Michigan 49008-5252, USA*
[2]*Physics Division, Argonne National Laboratory, 9700 S. Cass Ave, Argonne Illinois 60439, USA*
[3]*Physics Department, Northwestern University, Evanston, Illinois 60208, USA*
[4]*Hebrew University, Jerusalem, Israel 91904*

(Received 17 September 2004; published 2 March 2005; publisher error corrected 10 March 2005)

We have studied the ^{2}H(^{8}Li, p)^{9}Li reaction to obtain information on the spins, parities, and single-neutron spectroscopic factors for states in ^{9}Li, using a radioactive ^{8}Li beam. The deduced properties of the lowest three states are compared to the predictions of a number of calculations for the structure of ^{9}Li. The results of *ab initio* quantum Monte Carlo calculations are in good agreement with the observed properties.

DOI: 10.1103/PhysRevLett.94.082502 PACS numbers: 21.10.Jx, 21.10.Hw, 25.60.Je, 27.20.+n

Modern theoretical and computational methods have made great strides in the calculation of many properties of light nuclei from basic principles (so-called *ab initio* calculations). With interactions derived from fits to nucleon-nucleon scattering data and the binding energies of few-body systems, calculations using quantum Monte Carlo [1–3] and no-core shell-model (NCSM) [4,5] methods have been used to predict the binding energies, quantum numbers, charge and matter radii, and other properties of nuclei with $A \leq 12$. Many of these predicted properties are in good agreement with measured values. For most light systems, the existing knowledge comes largely from one- and few-nucleon transfer reactions. In many interesting cases, however, data are not available because the corresponding targets are unstable, and, until recently, information for many such nuclei has remained limited or out of reach. With the advent of radioactive nuclear beams, however, such studies can now be carried out by using inverse kinematics.

One such nucleus is ^{9}Li. Most of the available information on ^{9}Li comes from the ^{7}Li(t, p)^{9}Li reaction [6,7]. Other reactions, such as ^{9}Be(^{7}Li, ^{7}Be)^{9}Li [8] and ^{11}B(^{6}Li, ^{8}B)^{9}Li [9] have also been used. Only five levels are reported in the literature [6–11], and of these only one, the ground state, has a firm spin-parity assignment. This value, $3/2^{-}$, comes from the analysis of ^{9}Li β decay [12,13], and is consistent with the angular distribution in two-neutron transfer [6,7]. ^{9}Li is near the limit of current state-of-the-art "*ab initio*" calculations.

In this Letter, we report a study of the ^{2}H(^{8}Li, p)^{9}Li single-neutron transfer reaction. Reactions of this type are well known for their selectivity and their simplicity of interpretation, and have been used extensively in the past to study spins, parities, and single-particle spectroscopic factors for a variety of nuclei in the p shell [14]. The neutron spectroscopic factor is an experimental observable that has not yet been used as a test of the wave functions calculated using the theoretical frameworks described above. The goal of the current measurement is to obtain such spectroscopic factors for states in ^{9}Li.

Relatively few such measurements for transfer reactions utilizing unstable beams are reported in the literature [15–19]. Such studies present a number of experimental challenges. Difficulties include the low intensity of most radioactive beams and the choice of bombarding energy. To best interpret the (d, p) angular distributions obtained in such measurements, the optimal bombarding energy is between 4 and 10 MeV/nucleon. This energy range generally falls between the energy available from low-energy ISOL facilities (e.g., [16,17]), and from fragmentation facilities [18,19]. Furthermore, at the bombarding energies where (d, p) transfer is best understood, the protons emitted at forward center-of-mass angles, corresponding to backward angles in the laboratory, have low energies and are difficult to detect. Also, the laboratory-energy separation between groups corresponding to different excitation energies becomes small, thus requiring measurements with good energy resolution.

The ^{8}Li beam was produced using the in-flight production facility of the ATLAS accelerator at Argonne National Laboratory [20]. The production reaction was ^{2}H(^{7}Li, ^{8}Li)p. A ^{7}Li beam with an energy of 80 MeV and an intensity of 45–55 pnA bombarded a LN_2 cooled gas cell kept at a pressure of 700 mbar. The cell windows were fabricated from Fe-Ni-Co alloy foils with an areal density of 1.9 mg/cm^{2}. The ^{8}Li beam, with an energy of approximately 76 MeV, was focused using a 6 T magnetic solenoid. These particles were separated from the much more intense ^{7}Li primary beam using a dipole magnet and slit system located downstream from the solenoid. The energy resolution of the beam was $\Delta E/E \sim 0.5\%$. The difference in mass-to-charge ratio m/q between primary and secondary beams permitted a complete elimination of the ^{7}Li at the target position. The emittance of the beam was determined primarily by the kinematics of the production reaction, with scattering in the foils of the production cell being

a relatively small component. The size of the ^{8}Li beam spot was fixed by a 3 mm $\times$ 5 mm rectangular collimator at the entrance of the scattering chamber. Typically, the ^{8}Li intensity was 4–5 $\times$ 10^4 particles per second. The relative and absolute beam intensities were determined as described below.

The ^{8}Li ions bombarded a deuterated polyethylene (CD_2) foil with an areal density of 540 μg/cm^2. The reaction products were detected using a collection of large-area silicon detectors, as shown in Fig. 1. The backward emitted protons were detected using three annular double-sided segmented silicon detectors, placed 16, 36, and 64 mm upstream of the target. The active area of each of these detectors was divided into a set of 16 1.5-mm wide rings on one side, and 16 wedge-shaped regions on the other. The inner and outer radii of these detectors were 24 and 48 mm; they subtended angles of $109° \leq \theta_{\rm lab} \leq 124°$, $126.5° \leq \theta_{\rm lab} \leq 146°$, and $144° \leq \theta_{\rm lab} \leq 159°$, respectively. The energy thresholds of the proton detectors were made as low as possible, ~400 keV, in order to retain sensitivity for all the known excited states in ^{9}Li, even at the most backward angles.

To ensure that the particles observed in the upstream detectors were actually the protons of interest, forward-going Li ions were detected in coincidence with protons using a large-area array of silicon ΔE-E detector telescopes placed 390 mm downstream of the target position. This array consisted of four wedge-shaped telescopes with 500 μm thick ΔE elements, and E elements with thicknesses between 1.0 and 1.5 mm, and subtended angles between 1.3° and 7.3° in the laboratory. Apart from four 8° wide insensitive regions from the mounting structure of these detectors, the ΔE-E array covered the full 2π azimuthal angle range. This coincidence requirement eliminated backgrounds from reactions on ^{12}C nuclei in the target, or from β decay taking place in the target. While not all Li fragments had enough energy to penetrate the first layer of the ΔE-E array, a measurement of the energy of these fragments was sufficient to identify the products of the ^{2}H(^{8}Li, p)^{9}Li* reaction. As the one- and two-neutron separation energies in ^{9}Li are 4.063 and 6.096 MeV, respectively, protons populating excited states above these thresholds were detected in coincidence with ^{8}Li and ^{7}Li ions, instead of ^{9}Li.

The relative intensity of the beam was monitored throughout the experiment using an additional silicon surface-barrier telescope placed beyond the forward ΔE-E array. This monitor telescope detected ^{8}Li ions scattered at an angle of 6° from a gold foil also placed downstream from the ΔE-E array. The absolute efficiency of the beam monitor was determined in dedicated calibration runs by comparing the yield of ^{8}Li ions scattered from a 113 μg/cm^2 gold foil placed in the primary target position with that of ions scattered from the second gold foil to the monitor detectors. The absolute beam intensity could be determined to approximately 5%.

To determine the kinematic coincidence efficiency of the experimental setup, we performed Monte Carlo simulations of the reaction, where all factors including insensitive regions in the forward ΔE-E array, nonworking segments in the proton detectors, and the finite size of the beam spot were taken into account. For the particle-bound states in ^{9}Li, the procedure was straightforward with the results depending chiefly on the geometry of the setup, but also on the finite beam-spot size. For the neutron-unbound states, the neutron decay of the excited state in ^{9}Li was also simulated. The calculated efficiency was most sensitive to the beam-spot size and neutron-emission recoil for events with protons emitted at the most backward laboratory angles.

For proton-Li coincidence events, the reaction Q value was determined from the energy and angle of the detected protons; the measured spectrum is shown in Fig. 2. Peaks corresponding to transitions to the ground-, first-, and second-excited states are apparent. While there is also some evidence for strength at higher excitation energies, the kinematic shift, detector resolution, and electronic threshold make it difficult to draw specific conclusions about this excitation-energy range. The resolution in excitation energy was approximately 400 keV, FWHM, and is dominated by a combination of beam-spot size and detector segmentation as verified by Monte Carlo simulations.

Angular distributions are presented in Fig. 3. From a simple shell-model point of view, one expects that the strongest states in a (d, p) reaction will be populated by $l_{\rm tr} = 1$ transitions, where $l_{\rm tr}$ is the transferred angular momentum. The measured angular distributions for all three levels are forward peaked in character and fall off at a rate consistent with $l_{\rm tr} = 1$.

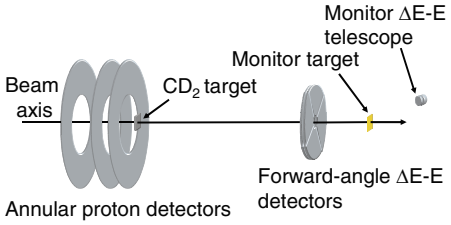

FIG. 1 (color online). Schematic diagram of the experimental setup.

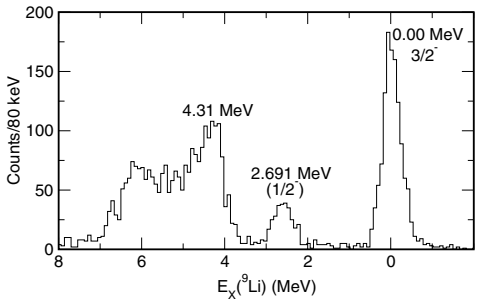

FIG. 2. Excitation-energy spectrum for ^{2}H(^{8}Li, p)^{9}Li. The sum of coincidences at all laboratory angles is shown.

Excitation energies and widths for the five reported levels in ^{9}Li are shown in Table I along with the first five states calculated from two standard shell-model interactions and two *ab initio* methods using realistic two- and three-nucleon potentials. The shell-model calculations are denoted by CK for the (6-16)2BME interaction of Cohen and Kurath [21], and DJM for the DJM69 interaction of Millener [22]. These results were obtained from older interactions using a model space limited to p-shell valence nucleons, and are included for historical completeness. Column GFMC gives results of Green's function Monte Carlo calculations for the AV18/UIX Hamiltonian [3], with Monte Carlo errors shown in parentheses; GFMC excitation energies calculated with the more realistic AV18/IL2 interaction are not statistically different. Column NCSM shows no-core shell-model results in a $4\hbar\omega$ basis for the AV8′/TM′(99) Hamiltonian [4,5]. The theoretical calculations all agree on the ordering of the states and roughly on their excitation energies. Positive parity states from a low-lying s orbital are known at low excitation in, e.g., ^{9}Be. Calculations for such states are uncertain in this region, and such an unbound level would possess a large neutron width. Table I also shows experimental spins, energies, and widths [11]; the experimental spin assignments include the results of the present work.

Total theoretical spectroscopic factors S(tot), defined by $S(\text{tot}) = S(p_{3/2}) + S(p_{1/2})$ are given in Table II for the CK, DJM, and NCSM calculations. Spectroscopic factors are not yet available from GFMC calculations, so we show the ones from the variational Monte Carlo (VMC) wave functions that serve as a starting point for the GFMC energy calculations [3]. The breakdown of the VMC spectroscopic factors into different $p_{1/2}$ and $p_{3/2}$ components are also given as they are used in the input to the distorted wave Born approximation (DWBA) calculations described below. The theoretical calculations for the first three states are generally in good agreement with each other. The strength of the second $3/2^-$ is less clear, however, all the models agree that the $7/2^-$ state will be only weakly excited, which is consistent with the small width of the fifth observed state.

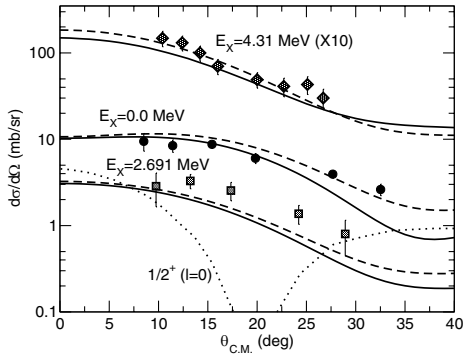

FIG. 3. Angular distributions for different states in ^{9}Li versus the c.m. (d, p) scattering angle. The curves show the absolute DWBA calculations described in the text. Note that the data and theoretical curves for the 4.31 MeV state are multiplied by 10.

The curves in Fig. 3 represent the absolute predictions of finite-range DWBA calculations performed with the program PTOLEMY [23] using $n + {}^8\text{Li}_{\text{g.s.}}$ form factors consistent with those obtained from spectroscopic overlaps calculated in the VMC framework described in [1–3]. Specifically, neutron form factors for the distorted wave calculations were obtained by calculating the wave function for a neutron bound with the experimental neutron binding energy in a Woods-Saxon (WS) potential, and adjusting the potential parameters so that the wave function is in good agreement with the one calculated using the VMC. Overlap wave functions and corresponding spectroscopic factors for both $p_{3/2}$ and $p_{1/2}$ transfer were computed and used in the DWBA calculations. Both s- and d-wave components of the AV18 deuteron [24] were also used for the (d, p) vertex, but the d-wave contributions were negligible. We have made a number of tests of this procedure for the ^{6,7}Li(d, p) stable-target reactions [14] and find agreement with the data within $\lesssim$30%. In the case of the $5/2^-$ level, which is unbound, the separation energy of the WS bound state was set at 0.2 MeV and the experimental Q value was used for the scattering wave functions. Tests showed that DWBA cross sections computed in this manner are unchanged if the separation energy is further lowered. Tests also showed that the DWBA calculations for all these states are sensitive to the overlap functions only beyond a ^{8}Li-n radius of $\sim$4.5 fm.

The solid and dashed curves in Fig. 3 represent the DWBA results obtained using the optical-model potential sets 1 and 2, respectively, from Ref. [14], with no additional normalization between the theory and the data. These potentials well reproduced the shapes of the forward angle data for neutron transfer on the $N = 5$ isotone of ^{8}Li, ^{10}B. Here, the shapes of the predicted distributions are in good agreement, and the magnitudes of the peak cross sections are in reasonable agreement, with data. These results are consistent with the accepted and tentative assignments of $J^\pi = 3/2^-$ and $1/2^-$ for $E_X = 0.00$ and 2.691 MeV, respectively. The unbound second-excited state is consistent with the theoretical expectation for a $J^\pi = 5/2^-$ level in Table I. Attempts to associate this peak with the other excited states shown in Tables I and II

TABLE I. Theoretical and experimental excitation energies for states in ^{9}Li.

	Theory					Experiment	
J^π	E_X (MeV)				J^π	E_X	Γ
	CK	DJM	GFMC	NCSM		(MeV)	(keV)
$3/2^-$	0.00	0.00	0.00	0.00	$3/2^-$	0.0	
$1/2^-$	3.33	1.54	1.5(4)	1.53	$(1/2^-)$	2.691	
$5/2^-$	3.88	3.23	3.0(5)	4.54	$(5/2^-)$	4.31	100(30)
$3/2^-$	5.45	4.28	3.6(5)	5.52		5.38	600(100)
$7/2^-$	6.57	5.63	5.7(4)	6.71		6.43	40

TABLE II. Theoretical and experimental spectroscopic factors for $n + {}^{8}\mathrm{Li}_{\mathrm{g.s.}} \rightarrow {}^{9}\mathrm{Li}$.

J^π	Theory						Experiment	
	CK	DJM	VMC		NCSM	(d, p)	Width
	S(tot)		$[S(p_{3/2})$	$S(p_{1/2})]$	S(tot)	S(tot)	S(tot)	S(tot)
$3/2^-$	0.90	0.92	[0.99	0.12]	1.11	1.05	0.90(13)	
$1/2^-$	0.20	0.47	[0.52	]	0.52	0.52	0.73(15)	
$5/2^-$	0.75	0.82	[0.18	0.60]	0.78	0.84	0.93(20)	0.55(30)
$3/2^-$	0.24	0.08	[0.10	0.32]	0.42	0.21		0.29(6)
$7/2^-$	0.0001	0.001	[0.009	]	0.009	0.002		0.0085(40)

require much larger renormalizations. In light nuclei, s states with $l_{\mathrm{tr}} = 0$ are possible; the shapes of the present angular distributions are inconsistent with $l_{\mathrm{tr}} = 0$, as shown by the dotted curve in Fig. 3. Experimental spectroscopic factors were determined by normalizing the absolute predictions in Fig. 3 to the forward angle data; the resulting values are listed in the "Experiment (d, p)" column of Table II. The uncertainties arise from the different values obtained using the different optical-model potentials and the uncertainty in the estimation of the normalization between theory and experiment.

An independent measure of the neutron spectroscopic factor for unbound levels can be obtained from an R-matrix analysis of the width of the state [25]. The reported widths of the three unbound states in ^{9}Li are also listed in Table I. Assuming $l_n = 1$, an R-matrix radius of 4.0 fm for the $^8\mathrm{Li} + n$ system, and $S(\mathrm{tot}) = \theta^2_{\lambda_c}$, the neutron spectroscopic factor for the second-excited state is 0.55(30). This and the corresponding values for the higher unbound levels are shown in the last column of Table II; they are in general agreement with the other values listed in the table. While the quality of the data above $E_X = 4.31$ MeV makes it difficult to draw detailed quantitative conclusions, it is possible that we see indications of the reported broad 5.38 MeV level, which might correspond to the expected second $3/2^-$ state shown in the tables.

In conclusion, we have studied the $^2\mathrm{H}(^8\mathrm{Li}, p)^9\mathrm{Li}$ reaction using a radioactive ^{8}Li beam in inverse kinematics. This work demonstrates that low-energy transfer experiments with radioactive beams in inverse kinematics can be used to extract quantitative spectroscopic information. This work also shows that such data can be used to test the predictions of *ab initio* model calculations of nuclear structure for nuclei away from stability, and that spectroscopic factors obtained from these calculations are in fact in good agreement with observation. From a comparison of the measured proton angular distributions with calculations performed using overlap wave functions and spectroscopic factors obtained from VMC calculations, we can strengthen the tentative $1/2^-$ assignment for the first excited state. We also tentatively assign $J^\pi = 5/2^-$ for the previously unassigned second-excited state at $E_X = 4.31$ MeV, providing new information about ^{9}Li and illustrating that similar studies are likely to be quite fruitful in the future.

This work was supported by The U. S. Department of Energy, Office of Nuclear Physics under Contract Nos. DE-FG02-04ER41320 (WMU), W-31-109-ENG-38 (ANL), DE-FG02-98ER4106 (NU), and the Faculty Research and Creative Activities Fund, Western Michigan University. The GFMC and VMC calculations were made with a grant of time on the Argonne National Laboratory Jazz computer.

[1] S. C. Pieper and R. B. Wiringa, Annu. Rev. Nucl. Part. Sci. **51** 53, (2001).
[2] S. C. Pieper *et al.*, Phys. Rev. C **64**, 014001 (2001).
[3] S. C. Pieper, K. Varga, and R. B. Wiringa, Phys. Rev. C **66**, 044310 (2002).
[4] P. Navrátil and B. R. Barrett, Phys. Rev. C **57**, 3119 (1998).
[5] P. Navrátil, Phys. Rev. C **70**, 054324 (2004).
[6] P. G. Young and R. H. Stokes, Phys. Rev. C **4**, 1597 (1971).
[7] F. Ajzenberg-Selove, E. R. Flynn, and O. Hansen, Phys. Rev. C **17**, 1283 (1978).
[8] R. B.Weisenmiller *et al.*, Nucl. Phys. **A280**, 217 (1977).
[9] Yu. A. Glukhov *et al.*, Yad. Fiz. **40**, 62 (1984).
[10] F. Ajzenberg-Selove, Nucl. Phys. **A490**, 1 (1988).
[11] D. R. Tilley *et al.*, Nucl. Phys. **A745**, 155 (2004).
[12] T. Lauritsen and F. Ajzenberg-Selove, Nucl. Phys. **78**, 1 (1966).
[13] Y. S. Chen, T. A. Tombrello, and R. W. Kavanagh, Nucl. Phys. **A146**, 136 (1970).
[14] J. P. Schiffer, G. C. Morrison, R. H. Siemssen, and B. Zeidman, Phys. Rev. **164**, 1274 (1967).
[15] K. E. Rehm *et al.*, Phys. Rev. Lett. **80**, 676 (1998).
[16] A. N. Ostrowski *et al.*, Nucl. Phys. **A701**, 621c (2002).
[17] N. de Sereville *et al.*, Phys. Rev. C **67**, 052801R (2003).
[18] A. A. Korsheninnikov *et al.*, Phys. Lett. B **343**, 53 (1995).
[19] P. Santi *et al.*, Phys. Rev. C **67**, 024606 (2003).
[20] B. Harss *et al.*, Rev. Sci. Instrum. **71**, 380 (2000).
[21] S. Cohen and D. Kurath, Nucl. Phys. **73**, 1 (1965); D. Kurath (private communication).
[22] J. Millener (private communication).
[23] M. H. Macfarlane and S. C. Pieper, Argonne National Laboratory Report No. ANL-76-11, Rev. 1, 1978.
[24] R. B. Wiringa, V. G. J. Stoks, and R. Schiavilla, Phys. Rev. C **51**, 38 (1995).
[25] A. M. Lane and R. G. Thomas, Rev. Mod. Phys. **30**, 257 (1958).